Chain Length Distribution and the Lamellar Crystal Structure of a Paraffin Wax

Douglas L. Dorset

Electron Crystallography Laboratory, Hauptman-Woodward Institute, 73 High Street, Buffalo, New York 14203-1196

Received: June 12, 2000; In Final Form: July 5, 2000

The three-dimensional crystal structure of an artificial linear paraffin wax with a near Gaussian distribution of chain lengths and known polydispersity (M_w/M_n) of 1.003 was determined from electron diffraction intensity data. The average structure resembles the paraffin n-$C_{35}H_{72}$ in its orthorhombic B-polymorph, space group $A2_1am$, where $a = 7.42$, $b = 4.96$, $c = 92.86$ Å. A distribution of fractional methylene group occupancies near the chain ends is suggested by the falloff of $I(00l)$ but a more accurate vacancy model can be found from the known chain distribution of this wax.

Introduction

Powder X-ray[1−4] and, more recently, single-crystal electron diffraction[5−9] investigations have provided important insights into the molecular associations in polydisperse paraffin chain assemblies of waxes and low molecular weight polyethylenes. There are at least two solid solution structures for normal chain assemblies—one with well-expressed lamellae[5] and the other with "nematocrystalline" disorder.[8,9] For waxes, the former lamellar expression is typical of a distillate fraction whereas the other type, where no true lamellar separation occurs, is typical of broader chain distributions of synthetic and natural products.

Following the extensive study of individual binary solid solutions in terms of average chain packing,[10] electron crystallography has provided an informative overview of representative wax assemblies in terms of their average single-crystal structures, most recently including three-dimensional determinations. Based on their crystal structures, petroleum distillate waxes are difficult to distinguish prima facie from *n*-paraffin binary solid solutions, although the defect distribution at the lamellar interface seems to depend on the breadth of the chain length distribution.[11] The nematocrystalline structures found for broad chain length distributions in synthetic Fischer−Tropsch waxes[8] and/or low molecular weight polyethylenes[9] and/or natural waxes[9] have also been characterized by electron crystallography, in addition to the microcrystalline waxes with a high concentration of methyl-branched chains.[7]

While respective crystal structure types can be useful for the classification of waxes, there is often little else that can be stated about a specific unknown wax, aside, perhaps from the "vacancy profile" at the lamellar interface.[11,12] In principle, the chain assembly of a wax can be modeled accurately only after its composition is well-characterized. This is particularly true because the polymethylene subcell repeat of the chain packing accounts for the most intense reflections of the diffraction pattern. Given such a sublattice array with small cell dimensions within a larger unit cell, the strong reflections are sequestered to restricted loci within the reciprocal lattice. The rest of the lattice comprises weak or unobserved reflections, which is also an informative part of the subcell Fourier transform. With the paucity of measured intensities, even in three-dimensional single-crystal patterns, there is often insufficient information to discern subtle features of the average composition just from a structure refinement.

In recent years the composition of representative petroleum-based waxes has begun to be accurately determined in terms of chain length distribution as well as the inclusion of branched and ring-substituted components.[13] To date, no effort has been made to construct chain packing models that conform to this compositional distribution, showing how these might improve the fit to measured electron diffraction intensity sets. In this paper, an artificial paraffin wax of known composition, with low polydispersity index, is described crystallographically in terms of the chain distribution.

Materials and Methods

Wax Construction and Crystallization. In a physical chemical characterization of artificial waxes at high pressure, Stokhuyzen and Pistorius[14] listed five approximately Gaussian mole fraction distributions of pure *n*-paraffin components as the materials used in their study, at least one of which could be grown into a single-crystal sufficient for X-ray diffraction data collection.[15] For this study, their highest molecular weight distribution, comprising chains from C31 to C39, was approximated by weighing out highly pure paraffins (various suppliers such as Fluka, Supelco, Eastman Chemical, and Ultra) from n-$C_{31}H_{64}$ to n-$C_{38}H_{78}$ on an analytical balance in the fractional distribution indicated in Figure 1. (The paraffin n-$C_{39}H_{80}$ was not available in our laboratory when this artificial wax was constructed. Nevertheless, it was not a major component of the original wax,[14] as seen in Figure 1.) After these paraffins were combined into a single vial, the physical mixture of crystals was melted, remixed, and then remelted several times to form a solid solution. Peak sharpness in the DSC scan (a 0.34 mg sample in a sealed aluminum pan scanned with a Mettler TA-3300 instrument) for this wax (Figure 2), henceforth termed STWX5 (*ST*okhuyzen *W*a*X* mixture *5*), indicated that the polydispersity index should be low,[11] as is also shown by calculation[16] from the known component molar distribution: $M_w/M_n = 1.003$. A premelting transition, presumably to a rotator phase, occurs at 68.6 °C, followed by the melt at 73.2 °C.

A small portion of the artificial wax was dissolved in light petroleum, and the sample was epitaxially crystallized on benzoic acid following procedures adapted from those described

10.1021/jp0021087 CCC: $19.00
Published on Web 08/05/2000

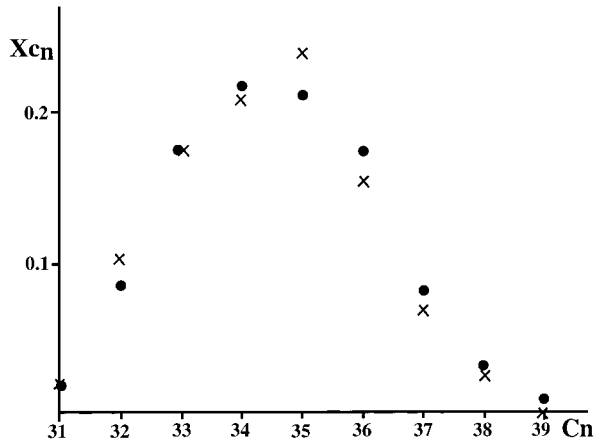

Figure 1. Mol fraction (X_{Cn}) distribution (×) of *n-paraffin*s C_n used to construct the model wax STWX5 in this study. The distribution (●) of a previous, similar model wax[14] is also shown.

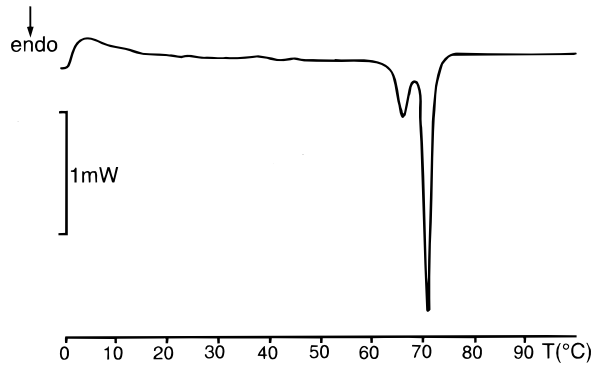

Figure 2. DSC scan of STWX5.

by Wittmann, Hodge, and Lotz.[17] Specifics of the preparation, which allow one to view directly crystalline projections containing the chain axes in electron diffraction experiments, are given in previous papers.[5−10] The epitaxial growth on the organic can be understood by the progression of crystallization events when a co-melt of the linear chain material in a suitable diluent is cooled into a eutectic solid, where the diluent (e. g., benzoic acid, naphthalene) is the major ingredient,[18] where there is no solid solubility of the two components. When the liquidus line of the phase diagram is crossed, the diluent crystallizes to form a flat crystal surface for nucleation of the chain molecules, that crystallize at a lower temperature when the solidus line is crossed. Close epitaxial matching of the surface crystal structure of the diluent with the lateral chain packing of the chains ensures that the chains are nucleated with their axes parallel to the diluent surface,[17] thereby nucleating a projection of the chain packing perpendicular to the one achieved by solution growth. After removal of the benzoic acid substrate by sublimation in vacuo, the oriented STWX5 samples on 300 mesh carbon-film-covered electron microscope grids could be studied in the electron microscope.

Electron Diffraction

Selected area electron diffraction studies of the oriented wax were carried out under low beam dose conditions[19] at 100 kV with a JEOL JEM-100CX II electron microscope. The selected area diameter, calibrated with a diffraction grating replica, was 2.9 μm. Three-dimensional data collection (Figure 3) was facilitated by use of a Gatan 650 Mk 1 sample holder with smooth, continuous 360° rotation of the specimen-containing grid at any tilt value of the ±60° eucentric goniometer stage.

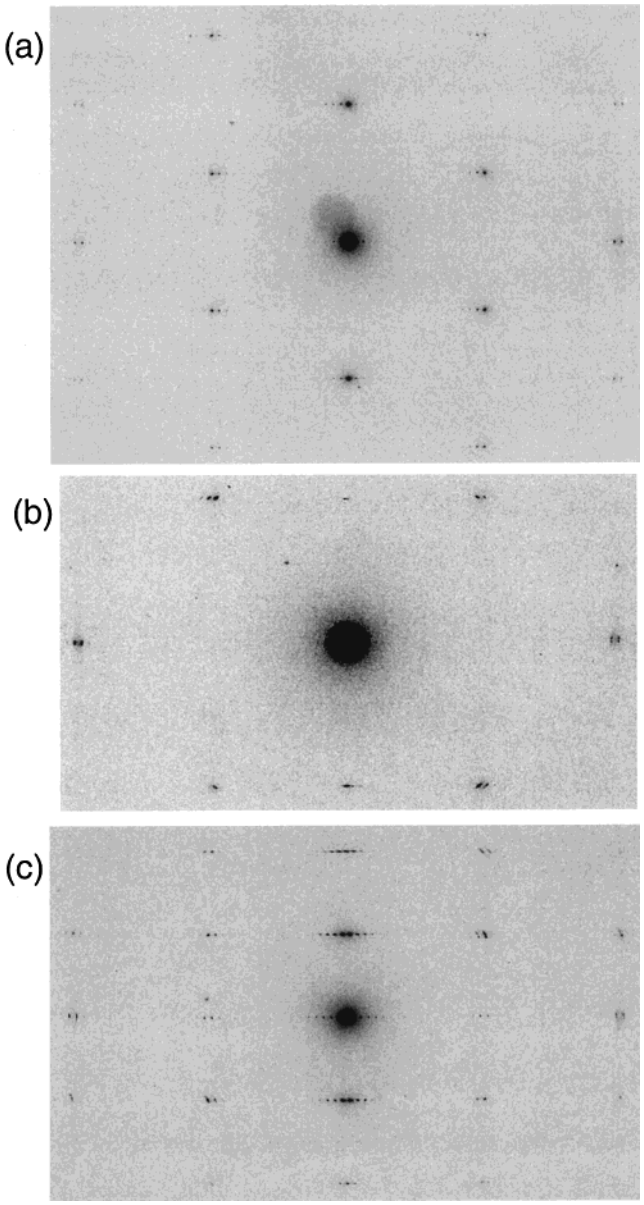

Figure 3. Electron diffraction patterns from epitaxially oriented STWX5. (a) 0k*l* (0° tilt); (b) h,2h,*l* (18° tilt), hh*l* (33° tilt).

The grids, tilted at various values (0° for the 0k*l* zone; 18° for the h,2h,*l* zone; 33° for the hh*l* zone), were rotated so that the specimen rod tilt axis coincided with the c* axis of the reciprocal lattice, permitting the collection of three-dimensional diffraction intensities (sampled by the indicated three major zone axis projections). All diffraction patterns were recorded on Kodak DEF-5 screenless X-ray film developed with Industrex developer at maximum strength (thus ensuring optimal film speed). The electron diffraction camera length was ultimately calibrated against a gold powder pattern but could also be evaluated from the d_{020} spacing of the orthorhombic methylene subcell packing,[20] which is very close to 2.48 Å.

Diffraction patterns were scanned on a Joyce-Loebl Mk IIIc flat-bed microdensitometer. Intensities of resulting peak traces were approximated by a triangular fit to the peak area. There was no Lorentz correction applied.[19] Many patterns were taken from the representative zonal projections, and efforts were made to ensure consistency of intensity data by comparing equivalent patterns as well as for symmetry-related reflections.[21] Intensity data from any projection, moreover, were built up as an average over several patterns and projections were scaled to one another

TABLE 1: Carbon Atom Coordinates for STWX5

x/*a*	*y*/*b*	*z*/*c*	x/*a*	*y*/*b*	*z*/*c*
0.037	0.190	0.0171	0.037	0.190	0.2644
0.119	0.309	0.0309	0.119	0.309	0.2781
0.037	0.190	0.0447	0.037	0.190	0.2918
0.119	0.309	0.0584	0.119	0.309	0.3055
0.037	0.190	0.0722	0.037	0.190	0.3193
0.119	0.309	0.0858	0.119	0.309	0.3330
0.037	0.190	0.0996	0.037	0.190	0.3468
0.119	0.309	0.1133	0.119	0.309	0.3604
0.037	0.190	0.1271	0.037	0.190	0.3742
0.119	0.309	0.1407	0.119	0.309	0.3879
0.037	0.190	0.1545	0.037	0.190	0.4017
0.119	0.309	0.1682	0.119	0.309	0.4154
0.037	0.190	0.1820	0.037	0.190	0.4291
0.119	0.309	0.1957	0.119	0.309	0.4428
0.037	0.190	0.2095	0.037	0.190	0.4566
0.119	0.309	0.2231	0.119	0.309	0.4703
0.037	0.190	0.2369	0.037	0.190	0.4841
0.119	0.309	0.2506			

via the intensities of strong wide-angle 00*l* reflections. Strong secondary scattering perturbations could be noted in some patterns, particularly the hh*l* zone in 00*l* rows, as also seen in previous studies of a pure paraffin.[22] Spuriously large intensities of this type were identified by their inconsistent occurrence and were therefore ignored.

Results

Indices of 0k*l*, h,2h,*l*, and hh*l* patterns followed the rule k + $l = 2n$ for observed reflections. Cell constants for a bilayer orthorhombic cell were determined to $a \approx 7.42$, $b \approx 4.96$, $c/2 = 46.43 \pm 0.26$ Å. Specifically, the indices of strong reflections were consistent to values expected[23] for a pure n-$C_{35}H_{72}$ paraffin in pseudoorthorhombic space group Aa or the orthorhombic $A2_1am$. (If the molecular mirror of the chains is used by the space group, the former assignment is equivalent to the latter.) Calculation of the lamellar repeat for this C35 alkane by Nyburg and Potworowski[24] matched the observed value exactly. Unlike some binary solid solutions[10] or polydisperse waxes,[5] there was very little deviation from the average C35 structure for this artificial STWX5 distribution.

The orthorhombic crystal structure of the odd-chain paraffins in the metastable B-polymorph is well-known.[23] A chain packing model based on C35 layers was accordingly constructed in space group Aa with an orthogonal β-angle to give the carbon fractional coordinates listed in Table 1. Using the Doyle−Turner electron scattering factor[25] for carbon and $B_C = 3.5$ Å^2, $R = \sum||\text{Fobs}| - k|\text{Fcalc}||/\sum|\text{Fobs} = 0.29$ for calculated and observed structure factors scaled (k) according to $\sum\text{Iobs} = \sum\text{Icalc}$ or 0.32 when the scale is based on $\sum|\text{Fobs}| = \sum|\text{Fcalc}|$. Unitary methylene group occupancy was assumed at all chain positions for this calculation. When theoretical hydrogen positions were added with $B_H = 5.5$ Å^2, again with unitary occupancies, $R = 0.24$ or 0.27, respectively. The average three-dimensional chain packing is represented in Figure 4. With crystallographic phases from the model structure factor calculation assigned to |Fobs|, an [100] projection of the lamellar packing was calculated as shown in Figure 5.

As has been often discussed and is indicated in Figure 5, the terminal methylene and methyl positions should not be given unitary occupancies for any sort of paraffin solid solutions. The resultant "vacancy distribution" actually denotes the presence of nonplanar conformational disorder[11,12,26] that accumulates near the chain ends, directly measurable by vibrational spectroscopy[27] or solid-state NMR.[28]

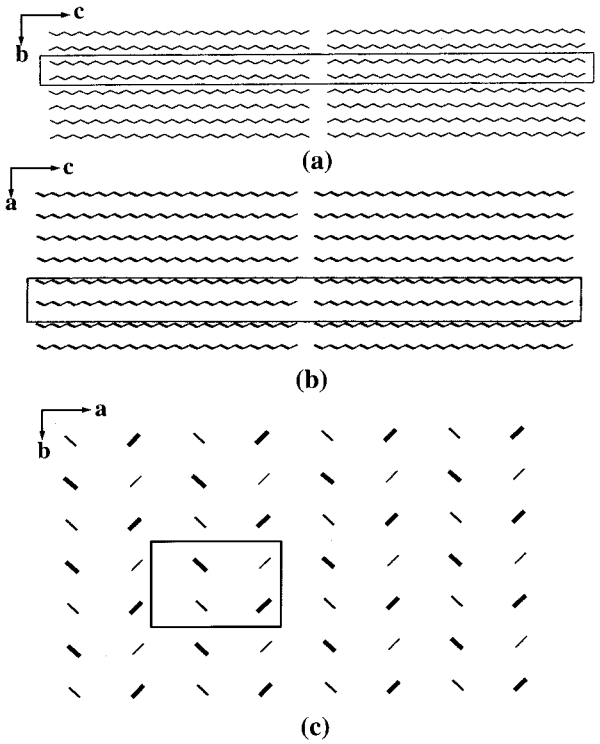

Figure 4. Three-dimensional packing of the average C35 length chain in STWX5. (a) [100] projection; (b) [010] projection; (c) [001] projection. In the latter, note the shift of adjacent lamellae (dark and light arrays are separate layers).

As originally introduced by Strobl and co-workers[26] for thermally disordered alkanes, but modified in a more recent study,[11] this distribution of vacancy sites can, in principle, be determined directly from the low-angle 00*l* intensity distribution, extrapolating to a zero scattering value by the fit of a quadratic function. A value was found for $d_s = L - 1.275\,(m - 1)$ where $L = c/2$ and m is the chain length (35 carbons). This was converted to $d_s' = d_s/2$, and determined to be 1.54 Å, in this example. A scale factor q was found then from $q = I_0/(d_s')^2$, where I_0 is the extrapolated zero-angle 00*l* intensity value for the pure *n*-paraffin chain packing. With the scaled 00*l* intensity values for STWX5, the zero-angle value I_0 was again determined by extrapolation; hence $d'_{av} = (I_0/q)^{1/2}$ can be calculated to give the one-dimensional vacancy distribution depth for this chain assembly, in terms of distance from the lamellar interface center. For STWX5, this value was found to be 3.50 Å. In the previous paper,[11] these distances were compared favorably to phenomenological Gaussian occupancy distributions $[1.0 - g(z)]$ for the final chain positions, where $g(z) = \exp(-a^2z^2)$. Here z is the Cartesian chain position along the z-axis and a is a constant. From the table in the original publication one could see that the approximate value should be near $a = (2.0\text{ Å})^{-1}$. The fractional occupancy factors for the terminal carbon positions were 0.49, 0.88, 0.99, 1.00... (writing from the final methyl to successive methylene groups into the chain and at each end of the chain) and gave residuals $R = 0.22$ or 0.24. Slightly better values were found when $a = (1.9\text{ Å})^{-1}$. The resultant distribution of fractional occupancies near a lamellar terminus is indicated in Figure 6.

Since the chain length distribution is accurately known for this model wax, a layer model could be constructed with fractional chain occupancies assuming that the chains were totally extended. For chain components that were less than the length of the C35 lamellar average, one starting position was given for each end of the lamella so that the shorter chain methyl

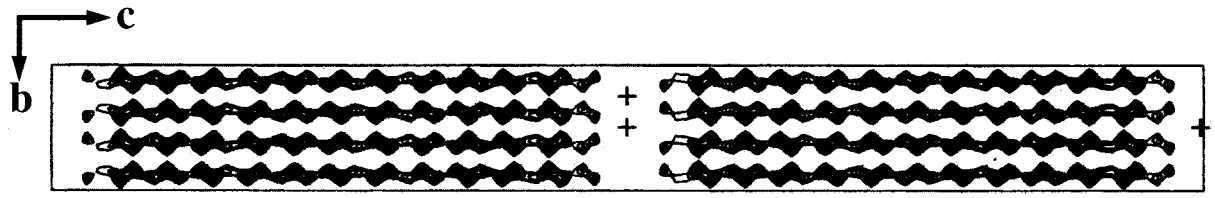

Figure 5. Potential map for STWX5 ([100] projection) showing partial group occupancies near the chain ends.

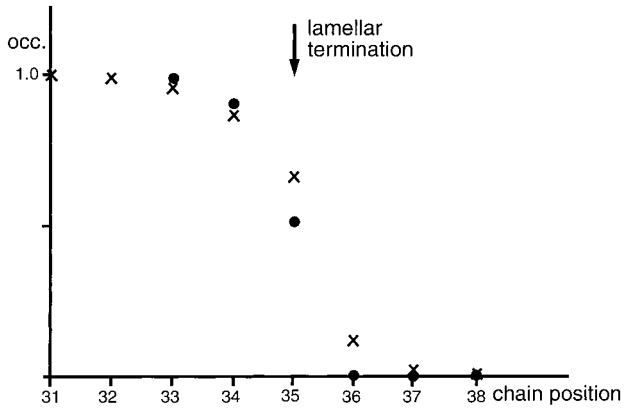

Figure 6. Occupancy parameters ("occ." on ordinate) for chain carbon atoms near one lamellar surface: (×) chain packing model from known distribution of components (Figure 1); (●) estimate from extrapolation of I(00*l*) to zero angle by the modified Strobl method.

group would be flush with the termination of the average lamella. Intermediate shifts of the chain by one carbon were then generated until the next position is found where the opposite methyl coincided with the opposite C35 lamellar surface limit. The occupancy of each of n chain positions for a given component i was then defined by $\sum_i x_i x_{in}$, where x_{in} is the fractional occupany for a given lamellar position n and x_i is the fractional molar contribution of component i. For chain components longer than the C35 average, one starting position was again generated with a methyl terminus at one lamellar surface and single methylene shifts were given to produce eventually the mirror image of this starting point, so that there was a similar partitioning of chains of this longer component i. In principle, with extended chains, this would place some chain termini outside the average lamellar boundary, as shown in the distribution for STWX5 in Figure 5. Within the C35 lamellar boundary the fractional occupancies were 0.67, 0.87, 0.96, 0.99, 1.00..., resulting in residual values 0.20 or 0.23. Calculated and observed structure factors are compared in Table 2.

TABLE 2: Observed and Calculated Structure Factor Magnitudes for STWX5

hk*l*	|Fobs|	|Fcalc|	hk*l*	|Fobs|	|Fcalc|
00 2	0.78	0.76	04 0	0.53	0.38
00 4	0.67	0.70	04 2	0.24	0.02
00 6	0.55	0.63	12 0	0.95	0.88
00 8	0.45	0.54	12 36	1.23	1.47
00 10	0.36	0.45	12 38	0.73	0.47
00 12	0.29	0.37	12 40	0.19	0.22
00 70	0.34	0.34	11 1	3.52	4.10
00 72	1.09	1.26	11 3	1.22	1.28
00 74	1.03	0.90	11 5	0.79	0.68
00 76	0.28	0.31	11 7	0.56	0.41
01 29	0.10	0.22	11 9	0.28	0.26
01 31	0.29	0.30	11 11	0.09	0.17
01 33	0.50	0.45	11 33	0.23	0.28
01 35	0.97	0.97	11 35	0.78	0.62
01 37	1.85	1.92	11 37	1.40	1.23
01 39	0.35	0.32	11 39	0.19	0.21
02 0	3.12	3.10	11 71	0.23	0.18
02 2	0.50	0.18	11 73	1.05	1.00
02 4	0.42	0.17	11 75	0.17	0.01
02 6	0.31	0.15	22 0	1.87	1.17
02 8	0.12	0.13	22 2	0.57	0.06
02 70	0.10	0.14	22 4	0.50	0.06
02 72	0.67	0.50	22 6	0.20	0.05
0 2 74	0.59	0.36	22 34	0.15	0.10
0 3 35	0.66	0.55	22 36	0.99	0.88
03 37	1.05	1.09	22 72	0.50	0.26
03 39	0.11	0.18	22 74	0.46	0.18

Discussion

As was found in a previous three-dimensional structure analysis of a refined paraffin wax with single-crystal electron diffraction intensities,[5] the artificial wax STWX5 crystallizes as a well-defined lamellar structure, closely resembling the structure of a pure odd-chain paraffin. Because of the low polydispersity of this wax, there is virtually no variation of the local average crystal structure on the scale of adjacent 3.0 μm diameter areas.

While a paraffin chain model incorporating fully occupied chain positions begins to explain the observed intensity data, it is also apparent that some kind of fractional occupancy distribution must be included within the chain termini to express the distribution of chain lengths in the structure. A vacancy distribution depth calculated by the modified Strobl method[26] successfully improves the fit of the model to the observed data. The resulting ratio $d'_{av}/d'_{s} = 2.27$ is very similar to the value found for a ternary paraffin solid solution[11] with two methylene groups difference between successive chain lengths. The number of observed (00*l*) orders observed for this ternary solid is also similar to the current result. However, a better fit can be obtained if the actual distribution of chain components is taken into account. However, the vacancy model was used only for carbon positions within the C35 boundary of the average lamellae, ignoring the implied (minor) protrusions into the interlamellar gap.

For such a model, if all chains were considered to be fully extended, this would place the fractional positions of three methylene units into a space that would conveniently accommodate only two methylenes,[9] again implying that the chains could also bridge across the lamellae. This, however, is not a simple proposition since successive lamellae are shifted with respect to one another in the x,y plane (Figure 3c). Therefore, some sort of conformational jog would be required to insert the chain protrusion into a (putative) vacancy site at the apposing lamellar surface.

In earlier X-ray crystal structures of a binary *n*-paraffin solid solutions,[29] such cilial projections into the lamellar interface were actually proposed. However, it was later shown that a packing model including an average lamellar surface that was atomically flat explained the X-ray data as well as the protruding chain model.[10] Decoration experiments with polymethylene vapors indicate that such surfaces, moreover, are good epitaxial substrates, also implying overall flatness.[10,30] Such a conclusion is also inferred (perhaps not conclusively) from AFM experiments on single paraffin solid solution lamellae.[30] That the

crystal growth in the [001] direction is highly correlated over micrometer lengths, i.e., a growth nucleated by the least ordered crystal plane in the structure, also indicates that this surface should be flat,[10] since average chain ends from one lamellar surface will face average interchain depressions of the facing layer, as described by Kitaigorodskii[31] for the lamellar layer stacking of pure alkane crystals.

Vibrational spectroscopy[27] detects the presence of nonplanar conformers at this surface. The calculated fractional occupancy of average chain position C36 protruding from a C35 lamella for the chain extended model is 0.13 whereas the fractional vacancy of C35 at the lamellar edge is 0.33 and that of C34 within the lamella is 0.13. It is clear that there is enough space on average within the lamellar surface to accommodate these terminal chain positions via nonplanar conformers, thus retracting the average chain length, so that they need not protrude into the interlamellar space. This structural feature is not easily established directly from diffraction measurements, even with single-crystal patterns, but it is the model that is most consistent with all observations, including the more direct spectroscopic measurements of chain disorder.[27,28]

While an improved model for the phenomenological vacancy distribution is obtained from a known chain distribution than from the vacancy depth analysis, there are questions that remain. For example, in waxes with a much higher polydispersity index,[11] will the approximation of using the anticipated vacancy distribution just within the defined limiting lamellar thickness still be superior to the vacancy depth analysis, especially if more chain mass is expected beyond the limiting lamellar surface?

Acknowledgment. Research was funded by grants from the National Science Foundation (CHE-9730317 and DMR-0071381) which are gratefully acknowledged.

References and Notes

(1) Craig, S. R.; Hastie, G. P.; Roberts, K. J.; Gerson, A. R.; Sherwood, J. N.; Tack, R. D. *J. Mater. Chem.* **1998**, *8*, 859; Craig, S. R.; Hastie, G. P.; Roberts, K. J.; Sherwood, J. N.; Tack, R. D.; Cernick, R. J. *J. Mater. Chem.* **1999**, *9*, 2385; Gerson, A. R.; Nyburg, S. C.; McAleer, A. *J. Appl. Crystallogr.* **1999**, 32, 296.

(2) Dirand, M.; Chevallier, V.; Provost, E.; Bouroukba, M.; Petitjean, D. *Fuel* **1998**, *77*, 1253.

(3) Retief, J. J.; Le Roux, J. H. *S. Afr. J. Sci.* **1983**, *79*, 234.

(4) Reynhardt, E. C.; Riederer, M. *Eur. Biophys. J.* **1994**, *23*, 59; Basson, I.; Reynhardt, E. C. *J. Phys. D. Appl. Phys.* **1988**, *21*, 1421, 1429, 1454.

(5) Dorset, D. L. *Acta Crystallogr.* **1995**, *B51*, 1021; Dorset, D. L. *Z. Kristallogr.* **1999**, *214*, 362.

(6) Dorset, D. L. *J. Phys. D. Appl. Phys.* **1997**, *30*, 451; Dorset, D. L. *J. Phys. D. Appl. Phys.* **1999**, *32*, 1276.

(7) Dorset, D. L. *Energy Fuels* **2000**, *14*, 685.

(8) Dorset, D. L. *J. Phys. Chem.* **2000**, *B104*, 4613.

(9) Dorset, D. L. *Macromolecules* **1999**, *32*, 162.

(10) Dorset, D. L. *Macromolecules* **1987**, *20*, 2782; Dorset, D. L. *Proc. Natl. Acad. Sci. U.S.A.* **1990**, *87*, 8541; Dorset, D. L. *Z. Kristallogr.* **1999**, *214*, 229.

(11) Dorset, D. L. *Z. Kristallogr.* **2000**, *215*, 190.

(12) Craievich, A.; Doucet, J.; Denicolo, I. *J. Phys. (Paris)* **1984**, *45*, 1473.

(13) Musser, B. J.; Kilpatrick, P. K. *Energy Fuels* **1998**, *12*, 715; Severin, D.; Gupta, A. K. *Petrol. Sci. Technol.* **1999**, *17*, 967; Gupta, A. K.; Brouwer, L.; Severin, D. *Petrol. Sci. Technol.* **1998**, *16*, 59; Coutinho, J. A. P.; Dauphin, C.; Daridon, J. L. *Fuel* **2000**, *79*, 607.

(14) Stokhuyzen, R.; Pistorius, C. W. F. T. *J. Appl. Chem.* **1970**, *20*, 1.

(15) Le Roux, J. H. *Fischer Tropsch Waxes*; Sasol One (Pty.) Ltd.: Sasolburg, South Africa, 1984; p 16.

(16) Billmeyer, F. W., Jr. *Textbook of Polymer Science*, 2nd ed.; Wiley-Interscience: New York, 1971; p 65−67, 78.

(17) Wittmann, J. C.; Hodge, A. M.; Lotz, B. *J. Polym. Sci. Polym. Phys. Ed.* **1983**, *21*, 2495.

(18) Dorset, D. L.; Hanlon, J.; Karet, G. *Macromolecules* **1989**, *22*, 2169.

(19) Dorset, D. L. *Structural Electron Crystallography*; Plenum: New York, 1995.

(20) Abrahamsson, S.; Dahlén, B.; Löfgren, H.; Pascher, I. *Prog. Chem. Fats Other Lipids* **1978**, *16*, 125.

(21) Dorset, D. L.; McCourt, M. P.; Li. G.; Voigt-Martin, I. G. *J. Appl. Crystallogr.* **1998**, *31*, 544.

(22) Hu, H. L.; Dorset, D. L.; Moss, B. *Ultramicroscopy* **1989**, *27*, 161.

(23) Dorset, D. L. *Z. Kristallogr.* **1999**, *214*, 223.

(24) Nyburg, S. C.; Potworowski, J. A. *Acta Crystallogr.* **1973**, *B29*, 347.

(25) Doyle, P. A.; Turner, P. S. *Acta Crystallogr.* **1968**, *A24*, 390.

(26) Strobl, G.; Ewen, B.; Fischer, E. W.; Piesczek, W. *J. Chem. Phys.* **1974**, *61*, 5257.

(27) Maroncelli, M.; Strauss, H. L.; Snyder, R. G. *J. Phys. Chem.* **1985**, *89*, 5260; Kim, Y. S.; Strauss, H. L.; Snyder, R. G. *J. Phys. Chem.* **1989**, *93*, 485; Clavell-Grunbaum, D.; Strauss, H. L.; Snyder, R. G. *J. Phys. Chem.* **1997**, *B101*, 335.

(28) Basson, I.; Reynhardt, E. C. *J. Chem. Phys.* **1991**, *95*, 1215.

(29) Lüth, H.; Nyburg, S. C.; Robinson, P. M.; Scott, H. G. *Mol. Cryst. Liq. Cryst.* **1974**, *27*, 337; Gerson, A. R.; Nyburg, S. C. *Acta Crystallogr.* **1994**, *B50*, 252.

(30) Dorset, D. L.; Annis, B. K. *Macromolecules* **1996**, *29*, 2969.

(31) Kitaigorodskii, A. I. *Organic Chemical Crystallography*; Plenum: New York, 1961; pp 193−204.